Variable Trial Functions and the CVBEM

T. V. Hromadka II
U.S. Geological Survey, Water Resources Division, Laguna Niguel, California

The Complex Variable Boundary Element Method, or CVBEM will be developed with respect to a variable trial function definition over each boundary element. The benefits in using this technique are that the modeling error in matching the prescribed boundary conditions (there is no error in satisfying the Laplace equation) is reduced without the addition of nodal points to the problem discretization. Consequently, the $n \times n$ matrix requirements are not increased when using this new approach.

INTRODUCTION

The Complex Variable Boundary Element Method, or CVBEM has been shown to be a valuable numerical technique for the analysis of two-dimensional potential problems. In Hromadka 1984 [1], several CVBEM applications are examined which include groundwater flow, St. Venant torsion, heat flow, ideal fluid flow, and other topics. Another reference which concentrates on the CVBEM development is Hromadka and Guymon 1983 [2], and includes a review of the pertinent background literature.

In this article, the CVBEM will be developed with respect to a variable trial function definition over each boundary element. The benefits in using this technique are that the modeling error in matching the prescribed boundary conditions (there is no error in satisfying the Laplace equation) is reduced without the addition of nodal points to the problem discretization. Consequently, the $n \times n$ matrix requirements are not increased when using this new approach.

CVBEM MODELING TECHNIQUE

In this section a brief review of the major concepts used in the CVBEM will be presented. Further details in developing a CVBEM model are provided in Appendix A.

The main objective of the CVBEM is to develop an approximation of the analytic function $\omega(z)$ where $\omega(z)$ is analytic over the simply connected domain Ω enclosed by the simple closed boundary Γ. Because $\omega(z)$ is analytic on $\Omega \cup \Gamma$, then

$$\omega(z) = \phi(z) + i\psi(z) \tag{1}$$

where $\phi(z)$ and $\psi(z)$ are the conjugate two-dimensional functions which both satisfy the Laplace equation over Ω.

Numerical Methods for Partial Differential Equations, 1, 259–278 (1985)
 CCC 0749-159X/85/040259-20$04.00

The CVBEM initiates by representing the problem boundary Γ as the union of m boundary elements by setting

$$\Gamma = \bigcup_{j=1}^{m} \Gamma_j \tag{2}$$

where each Γ_j is a straight line segment with nodal points specified at the end-points such as shown in Figures 1 and 2.

The next step in using the CVBEM is to develop a continuous approximation of $\omega(z)$ on Γ by the global trial function $G(z)$ where

$$G(z) = \sum_{j=1}^{m} N_j(z)\omega_j \tag{3}$$

where $N_j(z)$ is a continuous trial function representing the influence of ω_j over elements Γ_{j-1} and Γ_j; ω_j is the nodal point j value of $\omega_j = \omega(z_j) = \phi_j + i\psi_j = \phi(z_j) + i\psi(z_j)$; and $G(z)$ is defined for $Z \in \Gamma$. The CVBEM approximation function $\hat{\omega}(z)$ is developed by the line integral (taken in the counterclockwise direction)

$$\hat{\omega}(z) = \frac{1}{2\pi i}\int_{\Gamma} \frac{G(\zeta)\,d\zeta}{\zeta - z}, \qquad z \in \Omega. \tag{4}$$

Because $G(z)$ is continuous on Γ, then $\hat{\omega}(z)$ is also analytic over Ω and the real and imaginary parts of $\hat{\omega}(z)$ both satisfy the Laplace equation over Ω.

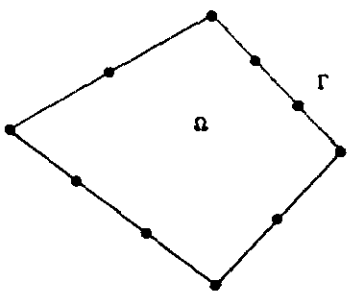

FIG. 1. Domain Ω and boundary Γ with nodal point placement.

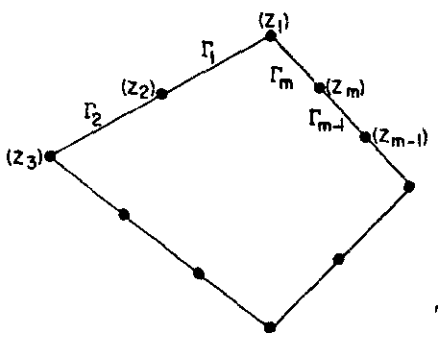

FIG. 2. Boundary element and nodal point definitions.

That is,

$$\hat{\omega}(z) = \hat{\phi}(z) + i\hat{\psi}(z), \qquad z \in \Omega \tag{5}$$

where

$$\nabla^2\hat{\phi}(z) = \nabla^2\hat{\psi}(z) = 0, \qquad z \in \Omega. \tag{6}$$

Previously, Hromadka 1984 [1] considered various polynomial trial functions on each Γ_j which resulted in CVBEM approximation functions analytic over Ω. Modeling error was evaluated by examining how well the CVBEM analog continuously matched the boundary conditions along Γ. At locations where large discrepancies were found, additional nodal points were added.

In this paper, modeling error will be attacked by redefining the trial function at locations on Γ where $\hat{\omega}(z)$ deviates substantially from the problem boundary conditions. In this fashion, the modeling error is reduced without the addition of nodal points on Γ (which is accompanied by an increase in the size of the fully populated CVBEM matrix system).

THE CVBEM NUMERICAL STATEMENT

The CVBEM model is a function of the 2m nodal values of $\overline{\phi}_j$ and $\overline{\psi}_j$ where $\overline{\omega}_j = \overline{\phi}_j + i\overline{\psi}_j$ is associated at node j. That is, if $\omega(z)$ is known at each node for $j = 1, 2, \cdots, m$, then the 2m nodal values of $\overline{\phi}_j$ and $\overline{\psi}_j$ are known on Γ and Eq. (4) results in the numerical statement

$$\hat{\omega}(z) = \hat{\omega}(z, \overline{\boldsymbol{\phi}}, \overline{\boldsymbol{\psi}}) \tag{7}$$

where $\overline{\boldsymbol{\phi}}$ and $\overline{\boldsymbol{\psi}}$ are the arrays of nodal values, and necessarily $\overline{\phi}_j = \phi(z_j)$ and $\overline{\psi}_j = \psi(z_j)$.

Generally, however, the problem boundary conditions only supply values for one of the functions $\phi(z)$ and $\psi(z)$ on portions of Γ. This situation results in many of the nodal points having one of the values $\overline{\phi}_j$ or $\overline{\psi}_j$ being an unknown. Thus, estimates for these unknown nodal values are needed in order to develop a CVBEM approximation, $\hat{\omega}(z)$.

Two approaches for estimating the unknown nodal values are provided as follows:

CLASS I: For each unknown nodal value, develop an explicit equation. For example, if $\overline{\phi}_j$ is unknown and $\overline{\psi}_j$ is known, define

$$\overline{\psi}_j \equiv \text{Im } \hat{\omega}(z_j) = \hat{\psi}(z_j, \overline{\boldsymbol{\phi}}, \overline{\boldsymbol{\psi}}) \tag{8a}$$

CLASS II: For each unknown nodal value, develop an implicit equation, that is from (8a),

$$\overline{\phi}_j \equiv \text{Re } \hat{\omega}(z_j) = \hat{\phi}(z_j, \overline{\boldsymbol{\phi}}, \overline{\boldsymbol{\psi}}) \tag{8b}$$

Both the CLASS I and CLASS II systems result in estimates for the unknown nodal values of $\omega(z)$, but the CLASS I system will result in $\hat{\omega}(z)$ matching the known nodal values whereas the CLASS II system will result in $\hat{\omega}(z)$ matching the estimated nodal values.

SOURCE OF MODELING ERROR

Should the choice of trial functions be correct, then necessarily $\hat{\omega}(z) = \omega(z)$ over Ω. Consequently, CVBEM modeling error occurs due to the trial functions being incorrect over boundary elements which have unknown nodal values.

To improve accuracy, nodal points may be added which result in an improved integration of the unknown function [e.g., $\phi(z)$ or $\psi(z)$] on a boundary element. The approach used in this article, however, is to redefine the trial function on the boundary element rather than add nodal points.

VARIABLE TRIAL FUNCTION DEFINITION

The problem boundary conditions will result in (at least) the specification of either $\phi(z)$ or $\psi(z)$ on each boundary element Γ_j. (Should both $\phi(z)$ and $\psi(z)$ be known on Γ_j, then $\omega(z)$ is known on Γ_j and there will be no error contribution from this boundary element.) The known function will result in an exact contribution from element Γ_j in the calculations of $\hat{\omega}(z)$ values. The unknown function on Γ_j, however, will result in modeling errors due to the incorrect trial function assumptions.

An adjustable trial function can be used for the unknown function on element Γ_j. Figure 3 shows the trial function geometry definitions. From the figure it is seen that (for example) $\phi(z)$ is approximated by a continuous function composed of straight-line segments. The analyst selects the weightings η_j^- and η_j^+ for each nodal point on Γ which results in a constant nodal value ϕ_j^- being specified over lengths of $\eta_j^{+l_j}$ in element Γ_j and $\eta_j^{-l_{j-1}}$ in element Γ_{j-1}. The net effect of these weightings is an increase in nodal value influence over the corresponding element. Additionally, the line segment geometries result in simple CVBEM computations for the development of the global matrix systems.

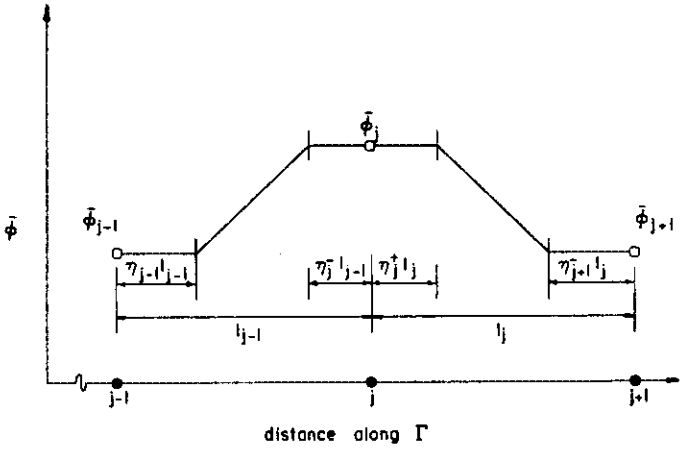

FIG. 3. Distribution of $\phi(z)$ on Γ.

BOUNDARY ELEMENT CONTRIBUTIONS

From Eq. (7), $\hat{\omega}(z)$ values depend on the boundary element contributions computed from the integral equation of (4). That is,

$$\hat{\omega}(z) = \sum_{j=1}^{m} \frac{1}{2\pi i} \int_{\Gamma_j} \frac{G(\zeta)\, d\zeta}{\zeta - z} = \sum_{j=1}^{m} I_j. \tag{9}$$

For element Γ_j, the total contribution is

$$I_j = \frac{1}{2\pi i} \int_{\Gamma_j} \frac{G(\zeta)\, d\zeta}{\zeta - z}. \tag{10}$$

If $\phi(z)$ is known on Γ_j, then a trial function can be selected to exactly calculate the $\phi(z)$ contribution for Γ_j. For $\psi(z)$ unknown on Γ_j, let the trial function be specified on Γ_j such as shown in Figure 4. Then the integral approximation is

$$\int_{\Gamma_j} \frac{\psi(\zeta)\, d\zeta}{\zeta - z} \simeq \int_{z_j}^{z_j^+} \bar{\psi}_j \frac{d\zeta}{\zeta - z} + \int_{z_j^+}^{z_{j+1}^-} \left[\frac{\zeta - z_j^+}{z_{j+1}^- - z_j^+}\right] \frac{\bar{\psi}_{j+1}\, d\zeta}{\zeta - z} + \int_{z_j^+}^{z_{j+1}^-} \left[\frac{z_{j+1}^- - \zeta}{z_{j+1}^- - z_j^+}\right] \frac{\bar{\psi}_j\, d\zeta}{\zeta - z} + \int_{z_{j+1}^-}^{z_{j+1}} \bar{\psi}_{j+1} \frac{d\zeta}{\zeta - z}. \tag{11}$$

The several components are directly calculated to be for element Γ_j as

$$\int_{\Gamma_j} \frac{\psi(\zeta)\, d\zeta}{\zeta - z} \simeq \bar{\psi}_j \left[\ln \frac{d_2}{d_1} + i\theta_1\right] + \bar{\psi}_{j+1} \left[1 + \left(\frac{z - z_j^+}{z_{j+1}^- - z_j^+}\right)\left(\ln \frac{d_3}{d_2} + i\theta_2\right)\right] - \bar{\psi}_j \left[1 + \left(\frac{z - z_{j+1}^-}{z_{j+1}^- - z_j^+}\right)\left(\ln \frac{d_3}{d_2} + i\theta_2\right)\right] + \bar{\psi}_{j+1} \left[\ln \frac{d_4}{d_3} + i\theta_3\right]. \tag{12}$$

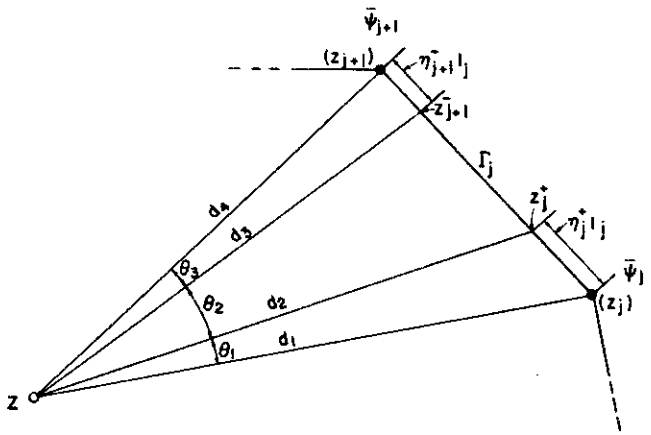

FIG. 4. Boundary element contribution geometry ($\psi(z)$ unknown).

Examination of (12) shows that the approximation is not defined should $z = z_j$ or z_{j+1}. In this case, the limiting value as $z \to z_j$ (for example) where $z \in \Omega$ is used and the Cauchy Principal Value results:

$$\lim_{z \to z_j} \int_{z_j^-}^{z_j^+} \bar{\psi}_j \frac{d\zeta}{\zeta - z} = \bar{\psi}_j \left(\ln \frac{d_6}{d_5} + i\theta \right), \qquad z \in \Omega. \tag{13}$$

From (12) and (13), the various nodal values (known and unknown) are multiplied by calculated complex numbers and summed together to form a global matrix system for the estimation of the unknown nodal values. Using the known and estimated nodal values, the CVBEM $\hat{\omega}(z)$ function is now available for use in modeling error analysis.

CVBEM ERROR ANALYSIS

Because the CVBEM develops a complex function $\hat{\omega}(z)$ which is analytic over Ω, the real and imaginary parts satisfy the Laplace equation exactly over Ω. Therefore, there is no error in satisfying the governing partial differential equation (Laplace equation). However, modeling error occurs due to $\hat{\omega}(z)$ not satisfying the boundary conditions continuously on Γ. This objective proceeds by first evaluating how $\hat{\omega}(z)$ values compare to the boundary conditions along Γ. Hromadka 1984 [1] presents several techniques for the evaluation and representation of this modeling error. The most convenient and easy-to-use technique was found to be the approximative boundary approach whereby a new boundary $\hat{\Gamma}$ is determined which represents the (x, y) coordinates where $\hat{\omega}(z)$ achieves the boundary condition values. Appendix B presents the main features of the approximative boundary technique.

Convergence of the CVBEM to the exact solution $\omega(z)$ can be shown by use of the unit circle.

For discussion purposes, let $u(z)$ be known continuously along the problem boundary C (Dirichlet problem) where C is the unit circle $C = \{z : |z| = 1\}$ which represents the transformation of the problem boundary Γ by use of the well known Schwarz-Christoffel theorem [3] and where $\omega^*(z) = u + iv$ is the corresponding transformation of $\omega(z)$. Then by the Poisson formula

$$v = -\frac{1}{2\pi} \int_C uW(\theta)\, d\theta \tag{14}$$

where $W(\theta)$ is the weighting function

$$W(\theta) = \frac{\sin \theta}{(1 = \cos \theta)}. \tag{15}$$

Figure 6 shows the distribution of $W(\theta)$ along C with respect to an arbitrary point $z_o \in C$ to reoriented to coincide with $\theta = 0$, where $-\pi < \theta \leq \pi$. Then use of the CVBEM necessarily involves the global trial function on C to approach $u(z)$ as the number of nodes increases. Hence, the error of approximation is defined by $e(z) = \omega^*(z) - \hat{\omega}(z)$ where $\hat{\omega}(z) = \hat{\phi} + i\hat{\psi}$ is the CVBEM approximation on C. Thus from (14),

$$v - \hat{\psi} = -\frac{1}{2\pi} \int_C (u - \hat{\phi}) W(\theta)\, d\theta \tag{16}$$

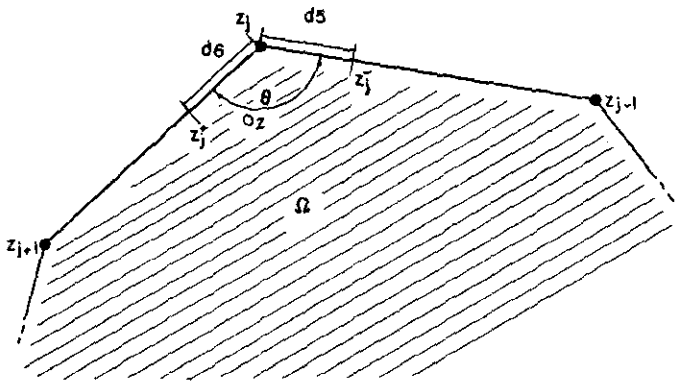

FIG. 5. Cauchy principal value case ($\psi(z)$ unknown).

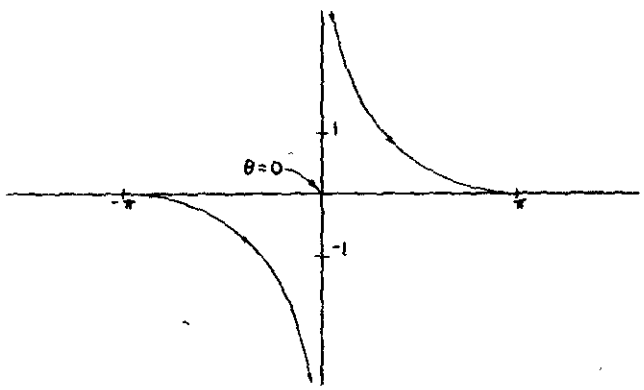

FIG. 6. The weighting function $w(\theta)$ for $z_o \in \Gamma$ (and $\theta = 0$).

and

$$|\nu - \hat{\psi}| \leq \frac{1}{2\pi} \int_C |(u - \hat{\phi}) W(\theta)\, d\theta| \tag{17}$$

The maximum error weighting occurs for $(u - \hat{\phi})$ distributed as shown in Figure 7. Thus for $|d(u - \hat{\phi})/dz|$ bounded by M, and $|u - \hat{\phi}| \leq E$, (17) is computed as

$$2\pi|u - \hat{\psi}| \leq 2E \int_\delta^\pi W(\theta)\, d\theta + 2 \int_0^\delta M\theta W(\theta)\, d\theta\,. \tag{18}$$

Solving the integrals,

$$2E \int_\delta^\pi W(\theta)\, d\theta = 2E[\ln 2 - \ln(1 - \cos\delta)] \tag{19}$$

and for E small,

$$2M \int_0^\delta \frac{\theta \sin\theta\, d\theta}{(1 - \cos\theta)} \to 2M \int_0^\delta \frac{24\, d\theta}{(12 - \theta^2)} \tag{20}$$

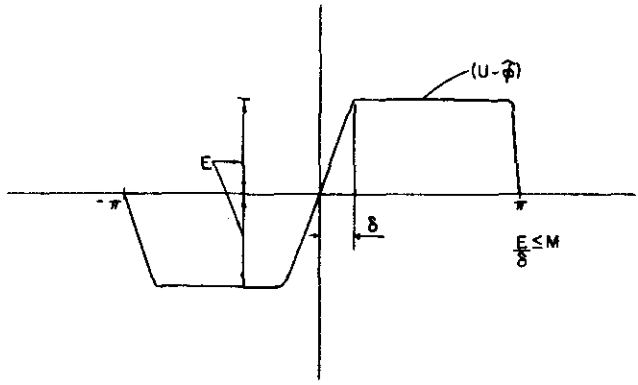

FIG. 7. Maximum error distribution along C with derivative bound M.

which for $\delta^2 \leq 4$, (20) reduces to

$$2M \int_0^{\delta} \frac{\theta \sin \theta \, d\theta}{(1 - \cos \theta)} \leq 12M\delta . \tag{21}$$

But from Figure 7, $\delta \geq E/M$ where $E = \max|u - \hat{\phi}|$ on C. Hence, the error of (17) is restated for E small

$$2\pi|v - \hat{\psi}| \leq 2E(\ln 2 - \ln \delta^2/2) + 12E \tag{22}$$

or rearranging terms

$$2\pi|v - \hat{\psi}| \leq 16E + 4E \ln M - 4E \ln E . \tag{23}$$

Thus as $\max |u - \hat{\phi}| \to 0$, necessarily $\max |v - \hat{\psi}| \to 0$. Indeed, from (23), the $\max |v - \hat{\psi}|$ is bounded by $\max |u - \hat{\phi}|$ which is known on C (and Γ).

ADAPTIVE INTEGRATION

To better meet the boundary conditions, the typical procedure is to add nodal points on Γ where error is computed to be large. In this article, however, error will be reduced by modifying the trial functions used to represent the unknown function distribution on Γ. That is, from Figure 3 values for weightings η_j^+ and η_j^- will be selected to redistribute the continuous trial function definition on Γ where boundary error is found to be large. In this fashion the CVBEM error is reduced without the need to add nodal points to Γ.

In the following example problems, the variable trial function technique will be used with the approximative boundary to develop CVBEM models of boundary value problems. The modeling process stops when the approximative boundary is sufficiently "close" to the true problem boundary. Usually the tolerance selected is the actual construction tolerance of the project.

The modeling process initiates by the specifications of nodal points along Γ such as shown in Figure 1. The CVBEM approximation $\hat{\omega}(z)$ is developed initially assuming zero weightings of both η_j^+ and η_j^- for each node j; that is,

straight line approximations are used between nodal values (see Fig. 3). An approximative boundary $\hat{\Gamma}$ is then developed such as described in Appendix B.

Comparisons of the approximative boundary $\hat{\Gamma}$ to the true problem boundary Γ indicates where approximation error is large and where the CVBEM trial functions need correction. At locations of high deviation between Γ and $\hat{\Gamma}$, nodal point weighting factors are added.

APPLICATION

Two-dimensional ideal fluid flow can be described mathematically by the Laplace equation. Of interest is the flow net associated to ideal fluid flow around a cylinder such as shown in Figure 8. Figure 9 shows the nodal point

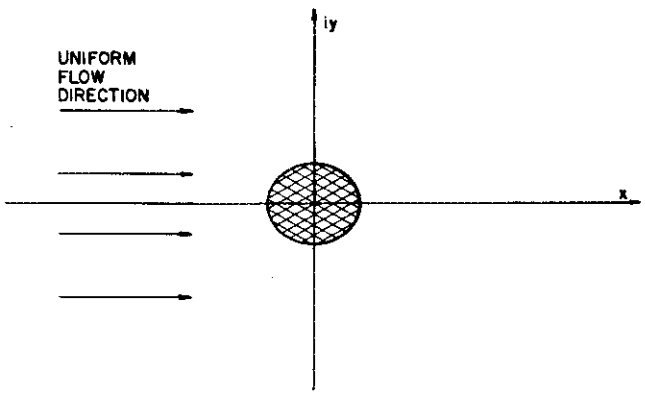

FIG. 8. Ideal fluid flow around a cylinder.

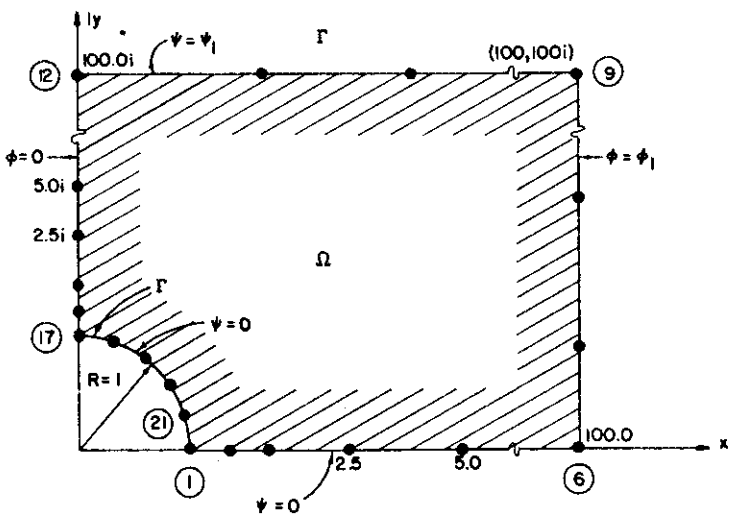

FIG. 9. Example problem nodal point placement.

placement where symmetry is used to reduce the problem domain expanse. Only the first quadrant is used, with 21 nodes defined on the problem boundary, Γ. Also shown are the boundary conditions (or level curves) assumed to represent the exact solution, $\omega(z)$ on $\Omega \cup \Gamma$.

The numerical solution is first based on weighting factors set at $\eta_j = 0.50$. This corresponds to a constant nodal value (for the unknown function) being defined over each boundary element. The approximative boundary corresponding to the boundary condition level curves is shown in Figure 10. From the figure, numerical integration error is most significant near the cylinder, and therefore, the trial function distribution requires the most adjustment.

To proceed, weightings of $\eta_j = 0$ are used (which corresponds to a linear trial function over each boundary element) and the corresponding approximative boundary is developed to investigate the amount of improvement in modeling accuracy. Based on this step, it was concluded that the trial function assumptions required adjustment near the intersection of the cylinder with the remaining problem boundary, i.e., near nodes 17 and 1 of Figure 9.

Figure 11 shows the trial function selected for use near the nodal points 1 and 17. From the figure, the trial function allows for an exceptional variation in unknown nodal values near the nodal point. The increase in computational accuracy is reflected in the closer fit between the approximative boundary $\hat{\Gamma}$ and the true problem boundary as shown in Figure 12.

IMPLEMENTATION

The procedure presented reflects the adaptive integration technique of reducing the integration errors due to the incorrect trial functions assumed for the unknown variable over each boundary element. This can be demonstrated by examining the CVBEM approximation of (4).

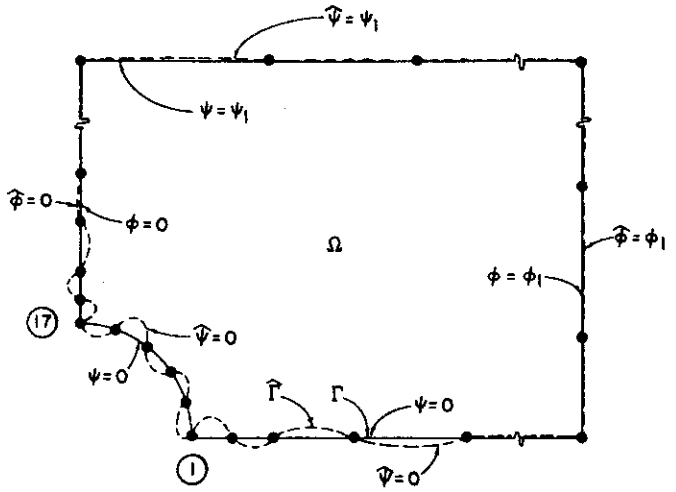

FIG. 10. Approximative boundary for $\eta_j^z = 0.50$.

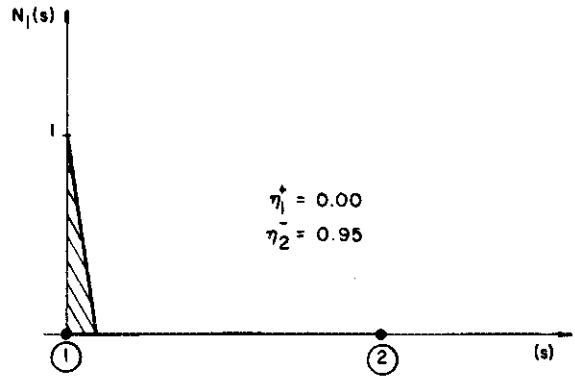

FIG. 11. Adjusted trial function for nodes ① (and ⑰).

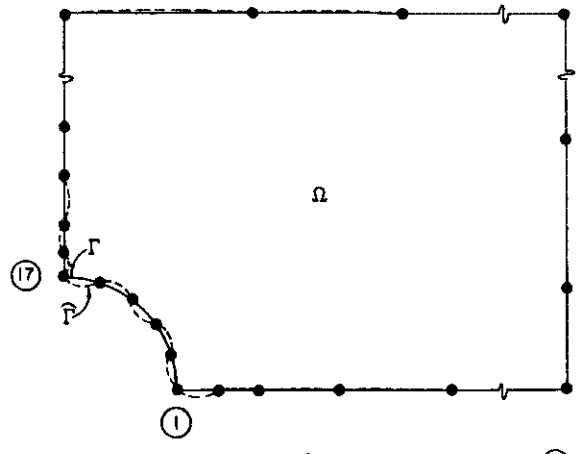

FIG. 12. Approximative boundary using $\eta_j^{\pm} = 0$ except for nodes ① and ⑰ (Node: displacements are magnified tenfold).

On each boundary element Γ_j, the true distribution of the solution is given by

$$\omega(\zeta) = G(\zeta) + e(\zeta), \qquad \zeta \in \Gamma \tag{24}$$

where over each element Γ_j,

$$\omega(\zeta) = N_j(\zeta)\omega(z_j) + N_{j+1}(\zeta)\omega(z_{j+1}) + e_j(\zeta), \qquad \zeta \in \Gamma_j. \tag{25}$$

In (25), $N_j(\zeta)$ and $N_{j+1}(\zeta)$ are linear trial functions, and $e_j(\zeta)$ satisfies the conditions

$$\left.\begin{aligned} &e_j(z_j) = e_j(z_{j+1}) = 0 \\ &e_j(\zeta) \equiv 0, \qquad \zeta \notin \Gamma_j \end{aligned}\right\}. \tag{26}$$

From the above, for each nodal location z_k,

$$\omega(z_k) = \frac{1}{2\pi i}\int_\Gamma \frac{[G(\zeta) + e(\zeta)]\,d\zeta}{\zeta - z_k} = \frac{1}{2\pi i}\sum_{j=1}^{m}\int_{\Gamma_j}\frac{G(\zeta)\,d\zeta}{\zeta - z_k} + \frac{1}{2\pi i}\int_{\Gamma_j}\frac{e(\zeta)\,d\zeta}{\zeta - z_k}. \tag{27}$$

Integrating the several terms of (27) determines the complex constant weightings w_{jk} where

$$\omega(z_k) = \sum_{j=1}^{m} w_{jk}\,\omega(z_j) + \sum_{j=1}^{m} e_{jk}. \tag{28}$$

It is noted in (28) that the complex constants w_{jk} are directly computed from integrating the $N_j(\zeta)$ functions with respect to each nodal coordinate z_k.

In (28), each complex nodal value can be written in terms of the known (boundary condition) value ξ_k and unknown (to be estimated) value ξ_u by

$$\omega(z_j) = \Delta\xi_k + \Delta\xi_u \tag{29}$$

where $\Delta = 1$ or i depending on the associated variable. Then (28) can be written in terms of the unknown nodal values as

$$\xi_u(z_k) = \sum_{j=1}^{m}\xi_u(z_j)W_{jk}^u + \sum_{j=1}^{m}\xi_k(z_j)W_{jk}^k + \sum_{j=1}^{m} e_{jk}^u \tag{30}$$

where the real contants W_{jk}^u and W_{jk}^k reflect whether $\xi_u(z_k)$ is the real or imaginary part of $\omega(z_k)$. In matrix form, (30) is expressed for m unknowns as

$$\boldsymbol{\xi}_u = \mathbf{N}_u\boldsymbol{\xi}_u + \mathbf{N}_k\boldsymbol{\xi}_k + \mathbf{E}_u. \tag{31}$$

where $\mathbf{N}_u$ and $\mathbf{N}_k$ correspond to the real constants W_{jk}^u and W_{jk}^k, respectively; $\boldsymbol{\xi}_u$ and $\boldsymbol{\xi}_k$ are the column vectors of nodal unknown and nodal known values, respectively; and $\mathbf{E}_u$ is the column vector of error contributions for each node.

In comparison, the CVBEM solves for the estimates $\hat{\boldsymbol{\xi}}_u$ of $\boldsymbol{\xi}_u$ by

$$\hat{\boldsymbol{\xi}}_u = \mathbf{N}_u\hat{\boldsymbol{\xi}}_u + \mathbf{N}_k\boldsymbol{\xi}_k. \tag{32}$$

Thus, error estimates for unknown nodal values are given by

$$(\boldsymbol{\xi}_u - \hat{\boldsymbol{\xi}}_u) = \mathbf{N}_u(\boldsymbol{\xi}_u - \hat{\boldsymbol{\xi}}_u) + \mathbf{E}_u \tag{33}$$

or

$$(\mathbf{I} - \mathbf{N}_u)(\boldsymbol{\xi}_u - \hat{\boldsymbol{\xi}}_u) = \mathbf{E}_u. \tag{34}$$

Letting $\mathbf{L} = \mathbf{I} - \mathbf{N}_u$ gives

$$\mathbf{L}(\boldsymbol{\xi}_u - \hat{\boldsymbol{\xi}}_u) = \mathbf{E}_u \tag{35}$$

where for row k of $\mathbf{E}_u$,

$$\|E_k\| = \left|\frac{1}{2\pi i}\int_\Gamma \frac{e(\zeta)\,d\zeta}{\zeta - z_k^*}\right| \le \frac{1}{2\pi}\int_\Gamma \frac{\|e(\zeta)\|\,|d\zeta|}{|\zeta - z_k^*|}. \tag{36}$$

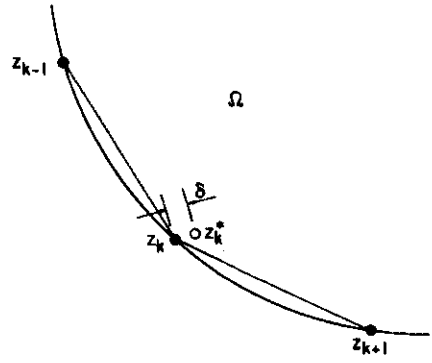

FIG. 13. Nodal position z_k^* for error estimate.

For $|\omega' - \hat{\omega}'| \leq M_1$ and z_k^* selected to be a distance $|z_k - z_k^*| = \delta$ from node z_k (see Fig. 13), (36) is evaluated as

$$\|E_k\| \leq \left(\frac{1}{2\pi}\right)\left(\frac{1M_1}{2}\right)\|\Gamma\|\left(\frac{1}{\delta}\right) \tag{37}$$

where $\|\Gamma\| = \int_\Gamma |d\zeta|$ and $1 = \|\Gamma\|/m$.
Thus, for contributions from elements Γ_{k-1} and Γ_k to row k of $\mathbf{E}_u$,

$$\|E_k\| \leq (\|\Gamma\|^2 M_1)/(2\pi m) \tag{38}$$

and $\|\mathbf{E}_u\| = \|E_k\| \to 0$ as $m \to \infty$.
Computational estimates of nodal accuracy are obtained by

$$\|\xi_u - \hat{\xi}_u\| \leq \|\mathbf{L}^{-1}\|\|\mathbf{E}_u\| \tag{39}$$

where $\|\xi_u - \hat{\xi}_u\| = \max_j |\xi_u(z_j) - \hat{\xi}_u(z_j)|$; $\|\mathbf{E}_u\|$ is given by (38); and $\|\mathbf{L}^{-1}\| = \max_j \sum_{n=1}^{m} |\mathbf{L}_{jn}^{-1}|$ where $\mathbf{L}_{jn}^{-1}$ are the matrix entries of $\mathbf{L}^{-1}$.

CONCLUSIONS

A new procedure for developing accurate CVBEM approximations is presented based on the definition of continuous trial functions over each boundary element. The technique is easy to use and the error analysis procedure is straightforward for linear programming. A significant benefit of this technique is that modeling error is reduced without the need for the addition of nodal points on the problem boundary.

APPENDIX A

Complex Variable Boundary Element Method

Hromadka and Guymon [2] present a detailed development of the CVBEM. A comprehensive presentation of the method is given in Hromadka, [1]. A feature available with the CVBEM is the generation of a relative error measure

which can be used to match the known boundary condition values of the problem. Consequently, the method can be used to develop a highly accurate approximation function for the Laplace equation and yet provide a descriptive relative error distribution for analysis purposes. Because the main objective of this article is to analyze the numerical error in solving (5), it is noted that the Laplace equation is solved throughout the problem domain (if homogeneous) or in connected subregions (if inhomogeneous). Many anisotropic effects can be accommodated by the usual rescaling procedures or by subdividing the total domain into easier-to-handle subproblems. The CVBEM is then applied to the problem domain(s) as discussed in the following.

Let Ω be a simply connected domain with boundary Γ where Γ is a simple closed contour (Fig. 14). Discretize Γ by m nodal points into m boundary elements such that a node is placed at every angle point on Γ (Fig. 15). Each boundary element is defined by

$$\Gamma_j = \{z : z = z(s) \text{ where } z(s) = z_j + (z_{j+1} - z_j)s, 0 \le s \le 1\}, \qquad j \ne m \tag{A1}$$

with the exception that on the last element,

$$\Gamma_m = \{z : z = z(s) \text{ where } z(s) = z_m + (z_1 - z_m)s, 0 \le s \le 1\}.$$

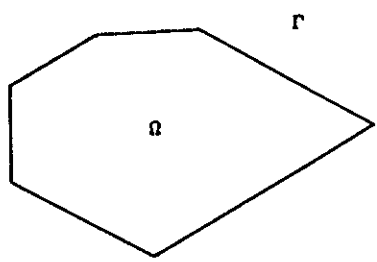

FIG. 14. Simply connected domain Ω with simple closed contour boundary Γ.

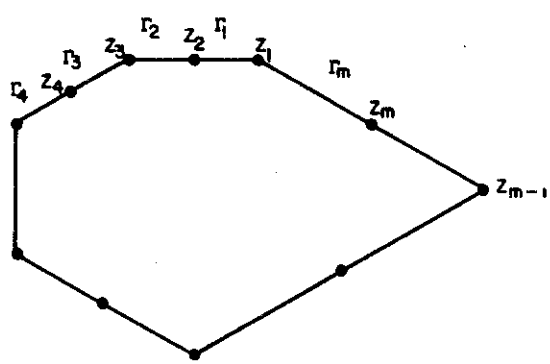

FIG. 15. Γ discretized into m boundary elements.

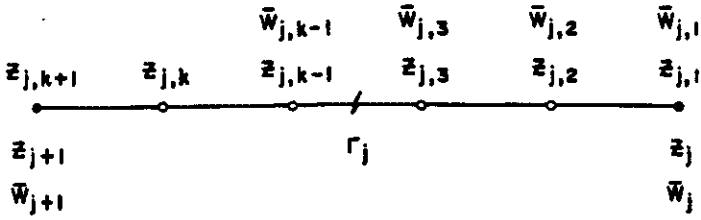

FIG. 16. $(k + 1)$-node boundary element Γ_j nodal definitions.

Then

$$\Gamma = \bigcup_{j=1}^{m} \Gamma_j \tag{A2}$$

Let each Γ_j be discretized by $(k + 1)$ evenly spaced nodes $(k \geq 1)$ such that Γ_j is subdivided into k equilength segments (Fig. 16). Then Γ_j is said to be a $(k + 1)$-node element. From Figure 16, each Γ_j has an associated nodal coordinate system such that $z_{j,1} = z_j$ and $z_{j,k+1} = z_{j+1} = z_{j+1,1}$.

On each Γ_j, define a local coordinate system by

$$\begin{aligned} \zeta_j(s) &= z_{j,1} + (z_{j,k+1} - z_{j,1})s, \qquad 0 \leq s \leq 1 \\ &= z_j + (z_{j+1} - z_j)s, \end{aligned} \tag{A3}$$

where $d\zeta_j = (z_{j,k+1} - z_{j,1})\,ds$.

On each $(k + 1)$-node element Γ_j, a set of order k polynomial basis functions are uniquely defined by

$$N_{j,i}^k(s) = a_{j,i,0} + a_{j,i,1}s + \cdots + a_{j,i,k}s^k, \tag{A4}$$

where $i = 1, 2, \cdots, (k + 1)$ and $0 \leq s \leq 1$, and where

$$N_{j,k}^k\left(\frac{z_{j,n} - z_{j,1}}{z_{j,k+1} - z_{j,1}}\right) = \begin{cases} 1, & n = i \\ 0, & n \neq i \end{cases}. \tag{A5}$$

The basis functions are further defined to have the property that for $\zeta \in \Gamma$

$$N_{j,i}^k\left(\frac{\zeta - z_{j,1}}{z_{j,k+1} - z_{j,1}}\right) = \begin{cases} N_{j,i}^k\left(\dfrac{\zeta - z_{j,1}}{z_{j,k+1} - z_{j,1}}\right), & \zeta \in \Gamma_j \\ 0, & \zeta \notin \Gamma_j \end{cases}. \tag{A6}$$

Let $\omega(z)$ be analytic on $\Omega \cup \Gamma$. That is, let $\omega(z)$ be the solution (unknown) to the steady-state boundary condition problem being considered. At each nodal point on Γ, define a specified nodal value by (Fig. 16)

$$\bar{\omega}_{j,i} = \omega(z_{j,i}) \tag{A7}$$

where from Fig. 16, $\bar{\omega}_{j,1} = \bar{\omega}_j = \bar{\omega}_{j-1,k+1}$.

Using (A6) and (A7), an order k global trial function is defined by

$$G^k(\zeta) = \sum_j G^k(\zeta_j(s)) = \sum_j \sum_{i=1}^{k} \overline{\omega}_{j,i} N_{j,i}^k \left(\frac{\zeta - z_j}{z_{j+1} - z_j} \right) \tag{A8}$$

From (A8), the global trial function is continuous on Γ. An H_k approximation function $\hat{\omega}_k(z)$ [1] is defined by the Cauchy integral

$$\hat{\omega}_k(z) = \frac{1}{2\pi i} \int_\Gamma \frac{G^k(\zeta)\, d\zeta}{\zeta - z}, \qquad z \in \Omega, \qquad z \notin \Gamma. \tag{A9}$$

Because the derivative of $\hat{\omega}_k(z)$ exists for all $z \in \Omega$, then $\hat{\omega}_k(z)$ is analytic in Ω and exactly solves the Laplace equation in Ω.

Expanding (A9) and using (A2) gives

$$\int_\Gamma \frac{G^k(\zeta)\, d\zeta}{\zeta - z} = \sum_{j=1}^{m} \int_{\Gamma_j} \frac{G^k(\zeta)\, d\zeta}{\zeta - z}. \tag{A10}$$

Integrating on boundary element j gives [1]

$$\int_{\Gamma_j} \frac{G^k(\zeta)\, d\zeta}{\zeta - z} = R_j^{k-1}(z) + \sum_{i=1}^{k} \overline{\omega}_{j,i} N_{j,i}^k(\gamma_j) \ln\left(\frac{z - z_{j+1}}{z - z_j} \right) \tag{A11}$$

where $R_j^{k-1}(z)$ is an order $(k - 1)$ complex polynomial resulting from the circuit around point z (see Fig. 17) and γ_j is equal to $(z - z_j)/(z_{j+1} - z_j)$. Thus, the CVBEM results in the approximation function

$$\hat{\omega}_k(z) = \frac{1}{2\pi i} \sum_j \left(R_j^{k-1}(z) + \sum_i \overline{\omega}_{j,i} N_{j,i}^k(\gamma_j) \ln\left(\frac{z - z_{j+1}}{z - z_j} \right) \right) \tag{A12}$$

or in a simpler form [1]

$$\hat{\omega}_k(z) = R^k(z) + \frac{1}{2\pi i} \sum_j \ln(z - z_j) \sum_i T_i^k \tag{A13}$$

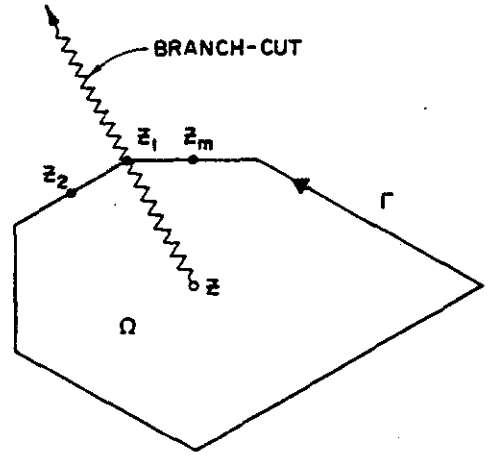

FIG. 17: Branch-cut of $Ln(z - \zeta)$ function, $\zeta \in \Gamma$.

where $T_i^k = \overline{\omega}_{j-1,i} N_{j-1,i}^k(\gamma_{j-1}) - \overline{\omega}_{j,i} N_{j,i}^k(\gamma_j)$, and $R^k(z)$ follows from (A12).

The approximation function of (A13) exactly satisfies the governing flow equation in the problem domain Ω for the approximated boundary conditions on the problem boundary, Γ. Because $\hat{\omega}_k(z)$ is analytic on Ω, then the maximum relative error of $|\omega(z) - \hat{\omega}_k(z)|$ must occur on Γ. Consequently, the total approximation error can be simply evaluated on Γ with the corresponding errors in the interior of Ω being less in magnitude. Because the boundary conditions used to evaluate (A13) are known continuously on Γ, then $\hat{\omega}_k(z)$ can be determined within arbitrary accuracy by the addition of nodal points on Γ due to (without proof)

$$2\pi i \lim_{\max|\Gamma_j|\to o} \hat{\omega}_k(z) = \int_\Gamma \frac{\lim_{\max|\Gamma_j|\to 0} G^k(\zeta)\, d\zeta}{\zeta - z} = \int_\Gamma \frac{\omega(\zeta)\, d\zeta}{\zeta - z} = 2\pi i \omega(z). \quad \text{(A14)}$$

APPENDIX B

The Approximative Boundary for CVBEM Error Analysis

Generally, the prescribed boundary conditions are values of constant ϕ or ψ on each Γ_j. These values correspond to level curves of the analytic function $\omega(z) = \phi + i\psi$. After determining a $\hat{\omega}(z)$, it is convenient to determine approximative boundary $\hat{\Gamma}$ which corresponds to the level curves of $\hat{\omega}(z) = \hat{\phi} + i\hat{\psi}$ which are specified as the prescribed boundary conditions. The resulting contour $\hat{\Gamma}$ is a visual representation of approximation error, and $\hat{\Gamma}$ coincident with Γ implies that $\hat{\omega}(z) = \omega(z)$. Additional collocation points are located at regions where $\hat{\Gamma}$ deviates substantially from Γ.

A difficulty in using this method of locating collocation points is that the contour $\hat{\Gamma}$ cannot be determined for points z outside of $\Omega \cup \Gamma$. To proceed, an analytic continuation of $\hat{\omega}(z)$ to the exterior is achieved by rewriting the integral function (A9) in terms of

$$\frac{1}{2\pi i} \int_\Gamma \frac{G(\zeta)\, d\zeta}{\zeta - z} = R_1(z) + \sum_{j=1}^{m} (\alpha_j + i\beta_j)(z - z_j)\, Ln(z - z_j), \quad \text{(B1)}$$

where α_j and β_j are real numbers; and $Ln(z - z_j)$ is a principle value logarithm with branch-cuts drawn normal to Γ from each branch point z_j such as shown in Figure 18. The resulting approximation is analytic everywhere except on each branch-cut. The $R_1(z)$ function in Eq. (B1) is a first order reference polynomial which results due to the integration circuit of 2π radians along Γ. If $\omega(z)$ is not a first order polynomial, then $R_1(z)$ can be omitted in (B1).

Implementation on a computer is direct although considerable computation effort is required. One strategy for using this technique is to subdivide each Γ_j with several internal points (about four to six) and determine $\hat{\omega}(z)$ at each point. Next, $\hat{\Gamma}$ is located by a Newton-Raphson stepping procedure in locating where $\hat{\omega}(z)$ matches the prescribed level curve. Thus, several evaluations of $\hat{\omega}(z)$ are needed to locate a single $\hat{\Gamma}$ point. However, the end product may be considered very useful since it can be argued that $\hat{\omega}(z)$ is the exact solution to the boundary

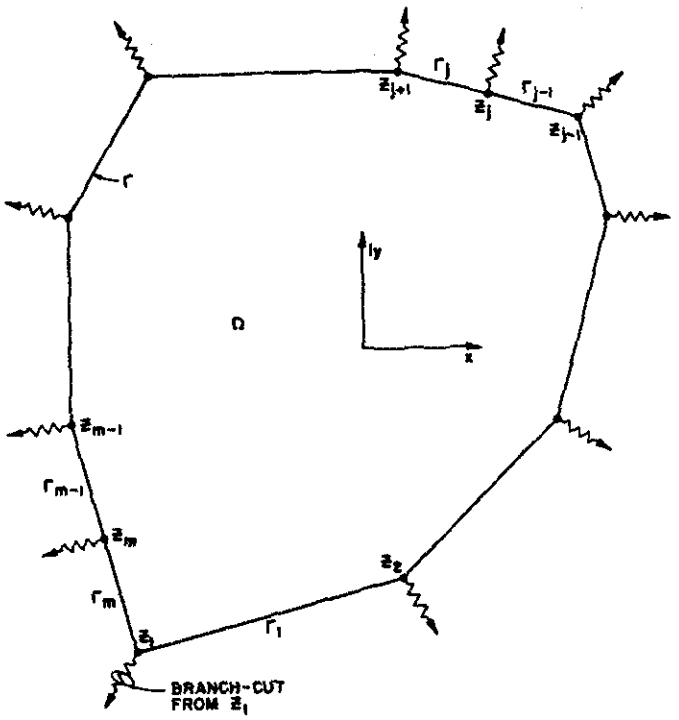

FIG. 18. The analytic continuation of $\hat{\omega}(z)$ to the exterior of $\Omega \cup \Gamma$. (note branch-cuts along Γ at nodes z_j).

value problem with Γ transformed to $\hat{\Gamma}$, and $\hat{\Gamma}$ is a visual indication of approximation error.

The use of the method discussed for locating additional collocation points on Γ is demonstrated by application of the CVBEM for solving two steady state heat transfer problems. The problems considered each involve a different geometry and set of boundary conditions of the Dirichlet class. The analytic solution to the problems are included in Figure 19. Each solution satisfies the Laplace equation and is defined as a function of a local coordinate x-y system with an origin specified as shown in the figures. On the problem boundaries, Γ, the potential function or temperature is also a continuous function of position defined by

$$\phi(z \in \Gamma) = \frac{1}{2}(x^2 + y^2). \tag{B2}$$

From (B2), it is seen that the boundary conditions are not level curves; consequently, the determination of an approximative boundary $\hat{\Gamma}$ requires further definition. In these applications, the problem is approached by using the statement

$$\hat{\Gamma} \equiv \left\{ z : \hat{\phi}(z) = \frac{1}{2}(x^2 + y^2) = \frac{1}{2}|z|^2 \right\}. \tag{B3}$$

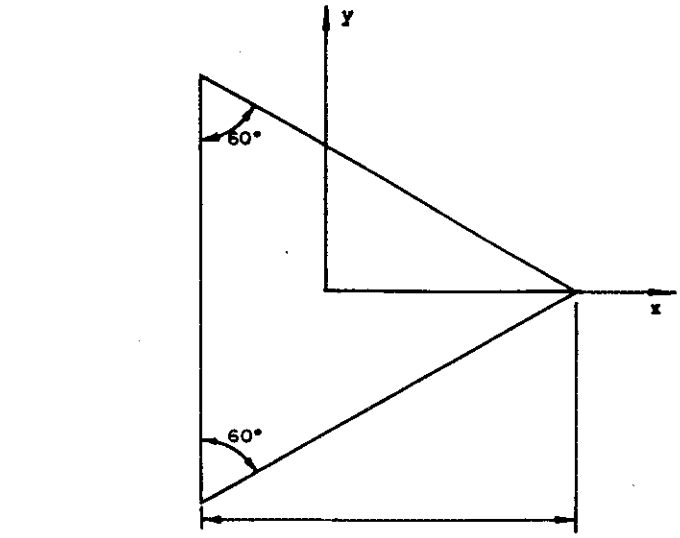

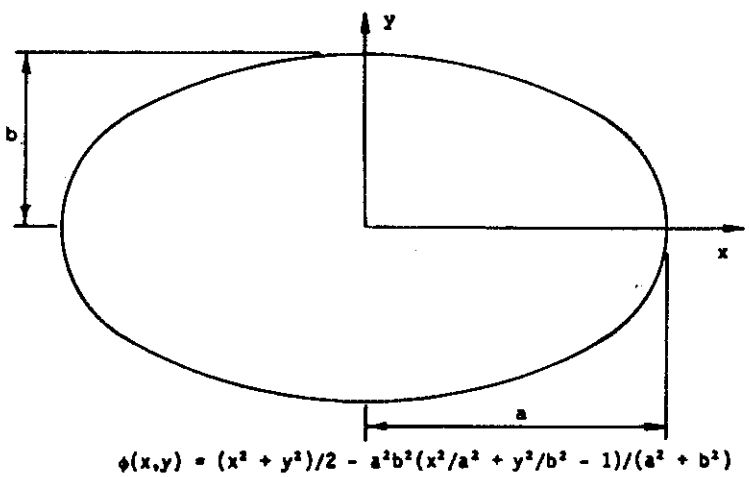

FIG. 19. Application problem geometrics and solutions for temperature, $\phi(x, y)$.

The strategy of working with level curves (i.e., $\phi = \phi_j$ for $z \in \Gamma_j$, $j = 1, 2, \cdots, m$) follows analogously.

The two applications illustrate the development of CVBEM approximation functions which exactly satisfy the governing partial differential equation (Laplace equation) in Ω and approximately satisfy the boundary conditions which are continuously specified on Γ. The subsequent figures illustrate the CVBEM error evaluations along Γ for evenly spaced nodal placements for each problem boundary.

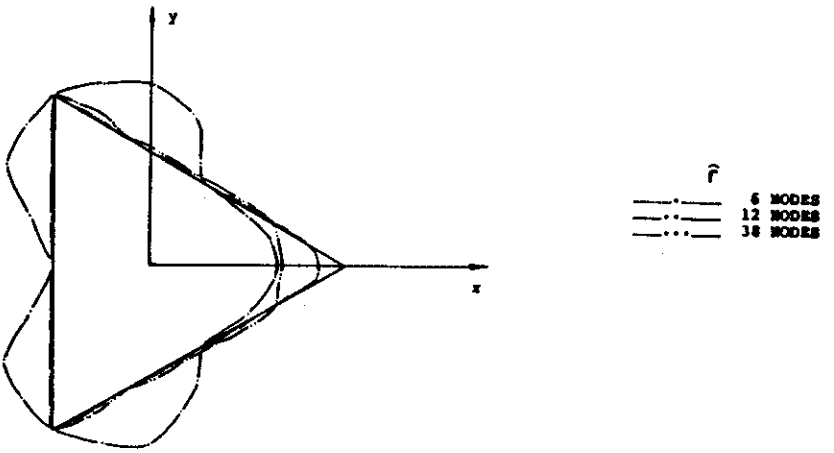

FIG. 20. Approximative boundaries for three nodal point distributions.

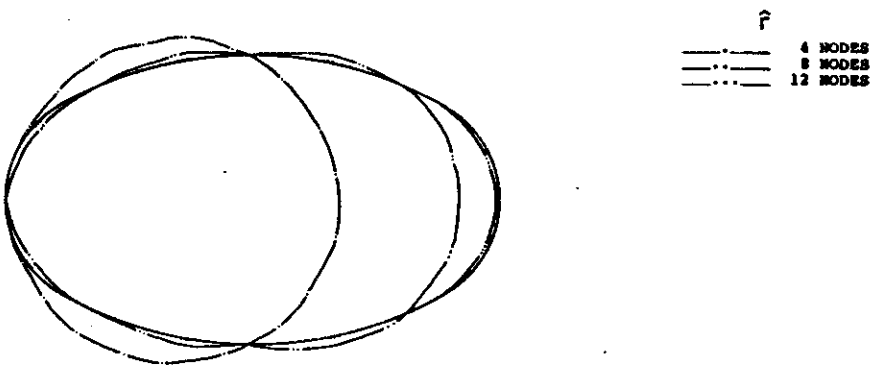

FIG. 21. Approximative boundaries for five nodal point distributions.

References

[1] T. V. Hromadka II, *The Complex Variable Boundary Element Method*, Springer-Verlag, 1984.

[2] T. V. Hromadka II, and G. L. Guymon, "The complex variable boundary element method: development," *Intern. Journal Num. Meth. in Eng.*, April, (1983).

[3] J. H. Mathews, *Basic Complex Variables for Mathematics and Engineering*, Allyn and Bacon, Inc., Boston, Massachusetts, 1982.